Three-Dimensional Fully π-Conjugated Macrocycles: When Truly 3D-Aromatic and when 2D-Aromatic-in-3D?

Ouissam El Bakouri [a,b], Dariusz W. Szczepanik [b,c], Kjell Jorner [a], Rabia Ayub [a], Patrick Bultinck [d], Miquel Solà*[b], and Henrik Ottosson*[a]

[a] Department of Chemistry - Ångström Laboratory, Uppsala University, Box 523, 751 20 Uppsala, Sweden. [b] Institut de Química Computacional i Catàlisi (IQCC) and Departament de Química, Universitat de Girona, C/ Maria Aurèlia Capmany 6, 17003 Girona, Catalonia, Spain. [c] K. Guminski Department of Theoretical Chemistry, Faculty of Chemistry, Jagiellonian University, Gronostajowa 2, Kraków 30-387, Poland. [d] Department of Chemistry, Ghent University, Krijgslaan 281 S3, 9000 Gent, Belgium.

Abstract: Recently, several fully π-conjugated macrocycles with strongly puckered or cage-type structures have been synthesized and found to exhibit aromatic character according to both experiments and computations. Herein, we examine their electronic structures and put them in relation to truly 3D-aromatic molecules (*e.g.*, *closo*-boranes and certain charged fullerenes) as well as 2D-aromatic polycyclic aromatic hydrocarbons. We use qualitative theory combined with quantum chemical calculations, and find that the macrocycles explored thus far should be described as 2D-aromatic with three-dimensional structures (*abbr*. 2D-aromatic-in-3D) instead of truly 3D-aromatic. Besides fulfilling the $6n + 2$ π-electron rule, 3D-aromatic molecules with highly symmetric structures (*e.g.*, T_d and O_h) have a number of molecular orbital (MO) levels that are (at least) triply degenerate. At lower symmetries, the triple (or higher) orbital degeneracies should be kept in approximate sense. This last criterion is not fulfilled by macrocyclic cage molecules that are 2D-aromatic-in-3D. Their aromaticity results from a

fulfillment of Hückel's 4*n* + 2 rule for each individual macrocyclic path, yet, their π-electron counts are coincidentally 6*n* + 2 numbers for macrocycles with three tethers of equal lengths. We instead link the 3D-macrocyclic molecules explored earlier to naphthalene, motivating their description as 2D-aromatics albeit with 3D structures. It is notable that macrocyclic cages which are 2D-aromatic-in-3D can be aromatic also when the tethers are of different lengths, *i.e.*, when their π-electron counts differ from 6*n* + 2. Finally, we identify tetrahedral and cubic π-conjugated molecules that fulfil the 6*n* + 2 rule and which exhibit significant electron delocalization. Yet, their properties are similar to those of analogous compounds with electron counts that differ from 6*n* + 2. Thus, despite that these tetrahedral and cubic molecules show substantial π-electron delocalization they should not be classified as true 3D-aromatics.

Introduction

Numerous unconventional forms of aromaticity have been identified experimentally in the last decades, *e.g.*, Möbius aromaticity in macrocycles and metallacycles,[1-6] all-metal σ-aromaticity in the solid state,[7] and aromaticity in electronically excited states.[8-16] Three-dimensional aromaticity (3D-aromaticity) is an intriguing topic introduced by Aihara in 1978 when he analyzed polyhedral boranes using a Hückel-type molecular orbital theoretical approach.[17] *Closo*-boranes, such as $[B_{12}H_{12}]^{2-}$ first synthesized in the late 1950s,[18] are now considered as 3D-aromatic and they are highly stable compounds.[19-23] Today, 3D-aromaticity is found in metal clusters and some charged fullerenes,[24-26] where the aromaticity of the latter is also classified as spherical aromaticity that follows Hirsch's $2(n+1)^2$ rule.[27] The tetrahedral P_4 molecule (white phosphorous) and Group 14 element E_4^{4-} Zintl ions have been labelled as 3D-aromatic,[28,29] and so has the Zn^I_8 ($Zn^I_8(HL)_4(L)_8^{12-}$, L = tetrazole dianion) metal cluster described as cubic aromatic since it exhibits an electron delocalization over the entire Zn^I_8 cube.[30] The unifying feature of these molecules is that they have a number of degenerate

molecular orbital (MO) levels which are at least triply degenerate, including the highest occupied and the lowest unoccupied MOs (HOMO and LUMO). We will henceforth call these molecules truly 3D-aromatic molecules.

The search for π-conjugated 3D-aromatic molecules and novel forms of aromaticity that extends in three dimensions is intense. One form of aromaticity in three dimensions, which recently has been labelled as 3D-aromaticity, is the through-space (face-to-face) aromaticity found in methano-bridged superphanes involving π-stacked [4*n*]annulenes and explored experimentally in cyclophanes and hexaphyrin dimers.[31-34] Another highly interesting and intriguing compound is the π-conjugated cage compound **1** (Figure 1) and its cations up to the hexacation $\mathbf{1}^{6+}$, which were reported by Wu and co-workers and considered to be "3D globally aromatic".[35] This bicyclic macrocycle consists of three equally long π-conjugated arms, and in its neutral form it was, according to computations, found to possess one Hückel aromatic cycle with 38π-electrons while the lack of aromaticity in the other two cycles is a result of the C_2 symmetric structure and poor π-conjugation in the third bridge. Yet, when the structure was enforced to D_3 symmetry the aromaticity supposedly involves the complete molecule. The same was found for $\mathbf{1}^{6+}$ which has a D_3 symmetric global minimum. Since the macrocycle **1** has 56 π-electrons, *i.e.*, a $6n + 2$ number ($n = 9$), and exhibits three diatropic ring-currents, it was concluded that **1** is 3D-aromatic when D_3 symmetric. This also applies to the hexacation which has 50 π-electrons, a $6n + 2$ number with $n = 8$. Subsequently, Casado and Martín considered **1** and its hexacation $\mathbf{1}^{6+}$ in terms of spherical aromaticity, and argued that the hexacation with 50 π-electrons follows Hirsch's $2(n + 1)^2$ rule for spherical aromaticity with $n = 4$.[36] However, here it should be realized that in D_3 symmetry the molecule has no other option than to exhibit three equivalent cyclic paths as the electronic structure must be symmetry-adapted.

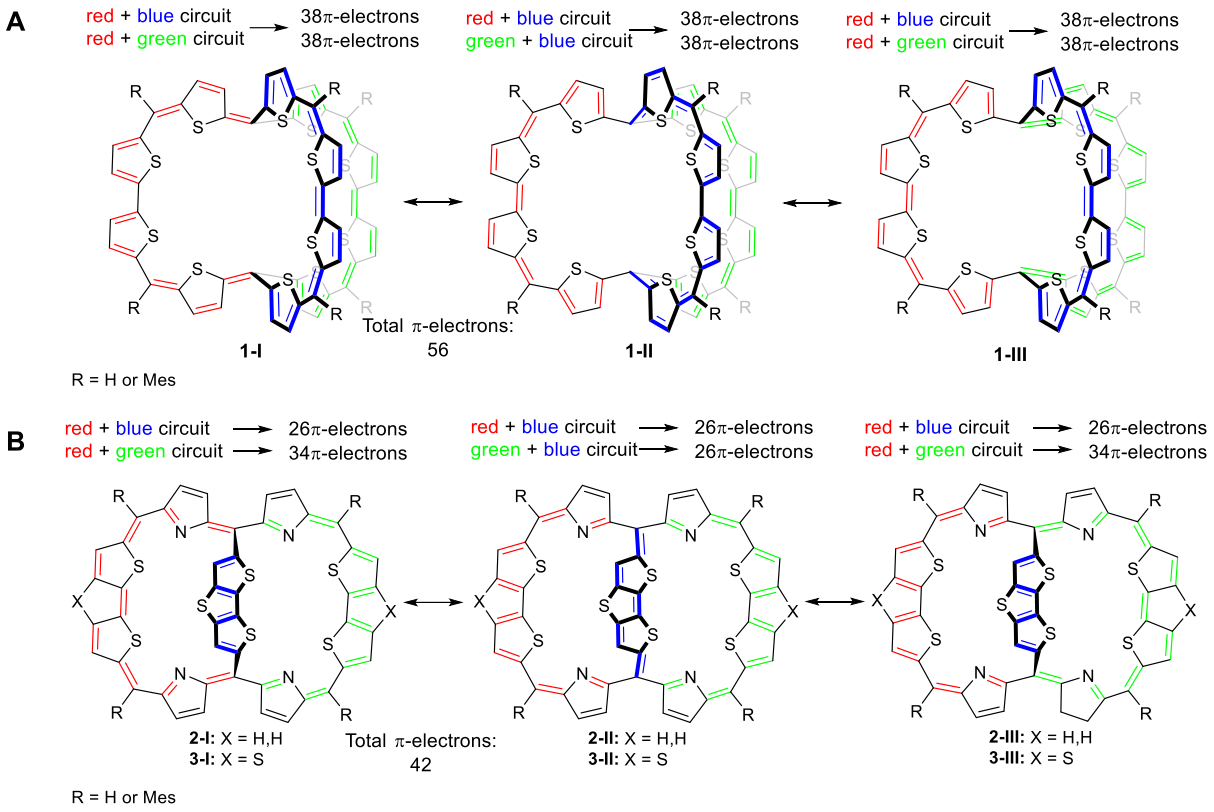

Figure 1: Three resonance structures of (A) the π-conjugated molecular cage **1**, and (B) non-planar dithienothiophene-bridged [34]octaphyrins **2** and **3** in their neutral forms. The totals of the π-electrons in the three circuits of **1** is 56 (a 6*n* + 2 number), while in **2** and **3** they are 42 (a 4*n* + 2 number) as counted by omitting the sulfurs from the main macrocycle conjugation pathway. The synthetized compounds have R = Mes substitution, yet, the computations herein were on parent compounds (R = H).

Earlier, a set of compounds related to **1**, the dithiopheno-bridged octaphyrins **2** and **3** (Figure 1) with structures that also expand in three dimensions, were explored by Kim and co-workers.[37] These compounds showed two diatropic ring currents with 26 and 34 π-electrons, respectively, a feature that the authors described as dual aromaticity. Yet, the authors also used the term bicycloaromaticity, a concept introduced by Goldstein in 1967 to describe through-space aromatic (homoaromatic) interaction in charged bicyclic macrocycles with puckered structures.[38] Results from ^{1}H NMR spectroscopy showed that the ring currents of **2** are

diatropic, and the aromatic character was further corroborated by Sundholm and co-workers through computations of magnetically induced current densities.[39] Compound **1** can be viewed as a further expanded version of **2** and **3** where the middle tether of the latter two has been expanded so that the three tethers become equivalent.

Clearly, most molecules are three-dimensional, but the mere combination of a 3D framework along with (aspects of) aromaticity is not a sufficient condition to label them as 3D-aromatic. As a simple example, helicenes are molecular scaffolds with 3D structures and they are aromatic, however, not 3D-aromatic. Instead, they have 2D-aromatic systems embedded in the 3D scaffolds. Compound **1** is also a three-dimensional framework and exhibits several characteristics of aromaticity, but does it satisfy the criteria to classify as a 3D-aromatic? Similarly, compounds **2** and **3** are bicyclic and aromatic, but are they bicycloaromatic? Is there another explanation for the observed aromatic characters? Considering that the essential features of true 3D-aromaticity and bicycloaromaticity are already described in the literature, how do compounds **1** – **3** and $\mathbf{1}^{6+}$ comply with these established definitions? Here it is noteworthy that the D_3 point group in **1** does not induce triply or higher-order orbital degeneracies, one of the main criteria of true 3D-aromaticity. Is the aromaticity in **1** – **3** and $\mathbf{1}^{6+}$ instead related to the Hückel-aromaticity of two-dimensional polycyclic aromatic hydrocarbons (PAHs)? Compounds **1** – **3** and $\mathbf{1}^{6+}$ are unusual and intriguing, yet, even though their aromatic character is apparent from both experimental and computational observations,[33,35,39] the cause of this aromaticity has not been analyzed in depth. In particular, there has been no search and investigation of macrocycles that potentially disprove the hypothesis that **1** and its hexacation comply with the $6n + 2$ rule for 3D-aromaticity and Hirsch's $2(n + 1)^2$ rule for spherical aromaticity. In this work we present a deeper theoretical analysis of **1** – **3** and related compounds, along with a computational analysis to establish the precise nature of the

aromaticity of these compounds. Such analyses will facilitate the future identification and design of three-dimensional π-conjugated compounds that are truly 3D-aromatic.

Results and Discussion

The analyses and discussions of our findings are split in two sections; a first with the qualitative theory on bicycloaromaticity, 3D-aromaticity, and 2D-aromaticity in three-dimensional compounds, and a second with computational results of these compounds discussed within the theoretical framework described in the first section.

Theoretical analysis: We start the theoretical analysis with the two dithiopheno-bridged octaphyrins **2** and **3** as they provide for a connection between PAHs and the cage-type macrocycles. Macrocycles **2** and **3** were recently labelled as bicycloaromatic,[35] a form of aromaticity defined by Goldstein as a case where three separate π-conjugated polyene segments (ribbons) in a bicyclic C_mH_m hydrocarbon interact through-space in either a longicyclic or a laticyclic topology (Figure 2).[40] Two criteria must be fulfilled for a bicycloaromatic interaction; (*i*) *m* must be an odd number (*i.e.*, odd number of C and H atoms), and (*ii*) the total number of π-electrons must equal 4*n*. With two isolating (sp^3 hybridized) bridgehead C atoms there will be *m* - 2 sp^2 hybridized C atoms in the polyene segments, and together with the two criteria, this implies that the bicycloaromaticity concept applies to cations and anions but not to neutral all-carbon species. An example of a potentially bicycloaromatic species is bicyclo[2.2.1]heptadienyl cation ($C_7H_7^+$) as it has four π-electrons and *m* = 7.[38] Conversely, bicyclo[3.2.2]nonatrienyl ($C_9H_9^+$) with *m* = 9 should in theory be bicycloantiaromatic as it has in total six π-electrons and the even-odd bridge interaction is destabilizing as it involves four π-electrons.

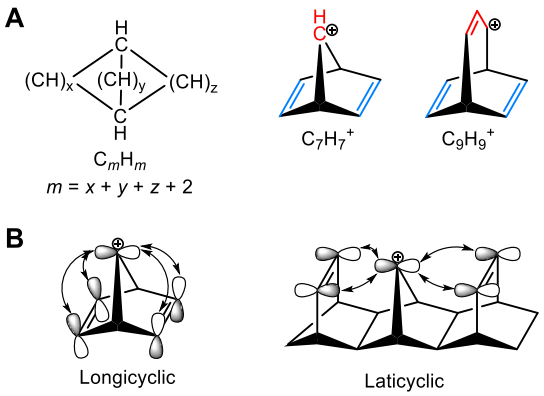

Figure 2: (A) General structure of a hydrocarbon that is bicycloaromatic and one example of a bicycloaromatic ($C_7H_7^+$) and a bicycloantiaromatic ($C_9H_9^+$) species. (B) Orbital interactions leading to bicycloaromatic stabilization in longicyclic and laticyclic topologies.

Based on the original definition of bicycloaromaticity, it is clear that **2** and **3** do not satisfy the criteria for bicycloaromaticity as (*i*) they possess 42 π-electrons (a $4n + 2$ number corresponding to bicycloantiaromaticity), (*ii*) the three bridges (ribbons) are not separate from each other as they all interact conjugatively with the two bridgehead atoms which are sp^2 instead of sp^3 hybridized, and (*iii*) all bridges have even numbers of atoms in the π-conjugated paths (16, 16 and 8) (Figure 1). With two bridgehead atoms this implies that they are not C_mH_m compounds with *m* being odd as the sum equals 42 (16 + 16 + 8 + 2). Thus, macrocycles **2** and **3** are not bicycloaromatic, although they are bicyclic and aromatic. The description of bicycloaromaticity by Kim and co-workers as a concept where "two (or more) potentially aromatic circuits are contained within the same non-planar molecular framework and share the same π electrons" is not in line with the original definition (Figure 2).

To determine if a compound is 3D-aromatic one should analyze its electronic structure. 2D-Aromaticity in D_{nh} symmetric all-carbon annulenic species (*e.g.*, benzene and the cyclopentadienyl anion) implies doubly degenerate HOMOs and LUMOs whereas in heteroaromatics with lower symmetries (*e.g.*, pyridine and pyrrole with C_{2v} symmetry) the

orbital degeneracies are lifted, although the orbital topologies are the same as in the highly symmetric isoelectronic all-carbon species. Similarly, an idealized 3D-aromatic species should have (at least) triply degenerate orbitals, but this degeneracy will be lifted when heteroatoms are incorporated in the molecular scaffold or when effects such as bond length alterations lower the symmetry. Indeed, Schleyer and co-workers concluded that the 4-center-2-electron 3D-aromaticity of the 1,3,5,7-bisdehydroadamantane dication manifests itself in a tetrahedral orbital topology, even though the molecule does not belong to the T_d point group.[41] 3D-Aromaticity is therefore preserved even if a highly symmetric geometric structure is distorted provided that the electronic structure remains similar. Now, are the aromatic features of **1** and $\mathbf{1}^{6+}$ in their D_3-symmetric geometries, together with their three-dimensional structures and $6n + 2$ π-electron counts, sufficient in order to categorize these species as true 3D-aromatics?

We argue that compounds **1** – **3** as well as $\mathbf{1}^{6+}$ are expanded and puckered versions of polycyclic aromatic hydrocarbons (PAHs) where the π-electrons are shared between a set of different circuits that each fulfil the $4n+2$ rule (Figure 3) (for **2** and **3** with different n).[42-47] The total ring-current picture of a PAH is constructed from all the different circuits that can be drawn. Naphthalene has three circuits; each hexagon (*a* and *b*) corresponds to a local six-electron circuit (A and B), while both hexagons are contained in the ten-electron circuit C. Furthermore, the induced diatropic ring-currents of circuits A and B, generated in an external magnetic field, are equivalent and cancel each other in the central C-C bond so that naphthalene exhibits an induced diatropic ring current exclusively along the perimeter. For anthracene there are six circuits (Figure 3), and upon a (weighted) summation of these it becomes apparent that the ring-current is concentrated to hexagon *b*. We now ask, to what extent is the aromaticity of the bicyclic macrocycles **2** and **3** similar to that of the bicyclic aromatic hydrocarbon naphthalene, *i.e.*, can **2** and **3** be labelled as expanded naphthalenes which have been puckered? Moreover, can naphthalene be altered/modified to the extent that its ring currents resemble

those of the two bicyclic macrocycles **2** and **3**? And are there not three aromatic cyclic paths in **2** and **3**?

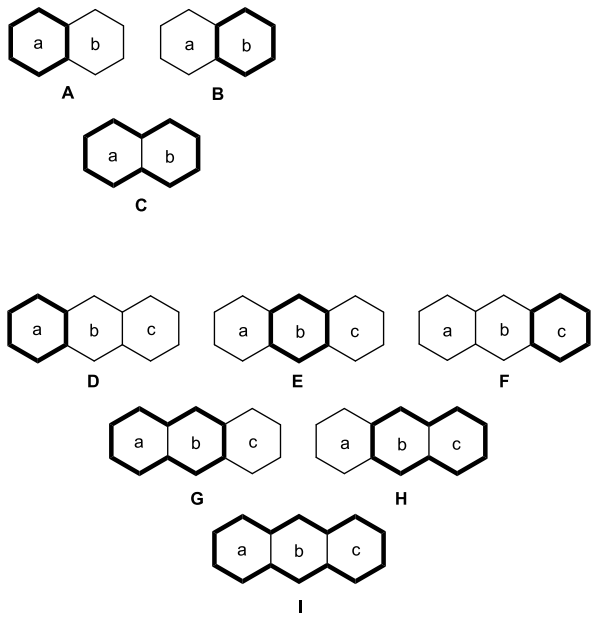

Figure 3: The three circuits of naphthalene and the six circuits of anthracene.

Figure 4A shows the two general bicyclic structures to which the three compounds of Wu, Kim and co-workers belong; the difference between the two structures being the total number of π-electrons in the three arms, *i.e.*, 4*n* (Type A) and 4*n* + 2 (Type B). Here it should be pointed out that the single π-electrons at the two bridgehead C atoms displayed in the generalized structures do not represent radical centers but instead indicate that these π-electrons are involved in π-bonds to either of the three linkers. Indeed, the three-dimensional bicyclic structures can all be viewed as expanded naphthalenes (Figure 4B). Starting at naphthalene we increase the π-electron count by expanding the six-membered rings through linkers while keeping the topology of Figure 4A to ensure that each circuit allows for 2D Hückel-aromaticity. The 1-[4.0.4]-1 label of naphthalene, used herein, reveals that there is one electron at each of the two bridgehead C atoms, four π-electrons in, respectively, the left and right linkers and none in the central, *i.e.*, naphthalene is a bicyclic Type A compound. Expanded naphthalenes are

obtained by incorporation of segments with, respectively, two or four π-electrons in each linker, leading to the Type B 1-[6.2.6]-1 and Type A 1-[8.4.8]-1 bicyclic molecules. Expanding the 1-[8.4.8]-1 Type A compound with a 1,3-butadiyne unit in the central linker gives a 1-[8.8.8]-1 Type A bicycle.

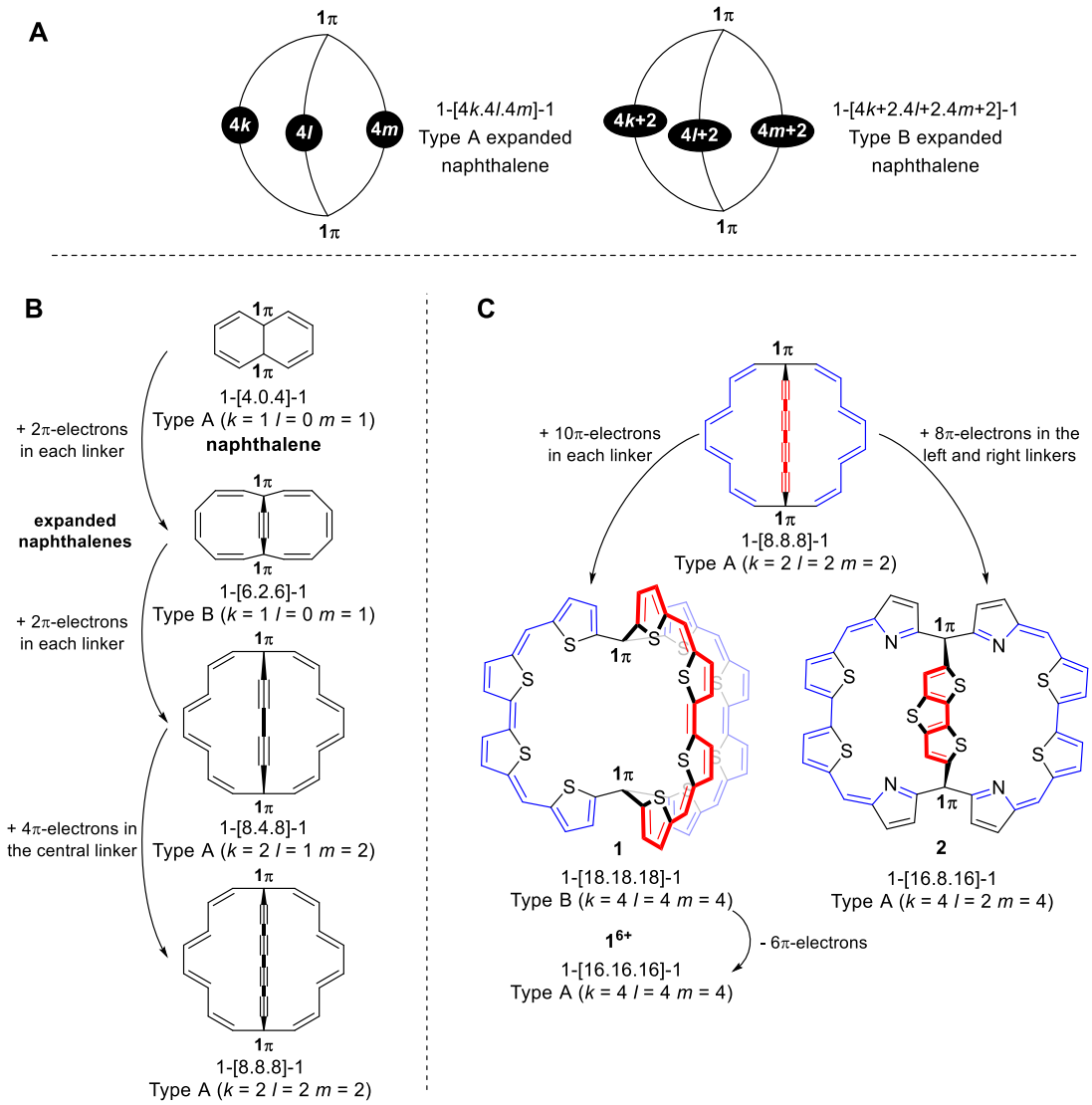

Figure 4: (A) Generalized descriptions of the three-linker bicyclic aromatic hydrocarbons labelled as Type A and Type B expanded naphthalenes. (B) Expansion of naphthalene to gradually larger three-dimensional bicyclic structures. (C) Application of the electron count approach for description of macrocycles **1**, $\mathbf{1}^{6+}$ and **2**. The number of π-electrons are derived by omitting the sulfurs from the main macrocycle conjugation pathway.

Starting at the 1-[8.8.8]-1 Type A compound, we expand the π-electron counts of the tethers to reach the three-dimensional macrocycles **1** – **3** (Figure 4C). As noted above, in its optimal geometry **1** has only one diatropic ring-current, a result of its C_2 symmetric structure where π-conjugation is significant in only one Hückel-aromatic cycle with 38 π-electrons. Yet, when enforced to D_3 symmetry, the molecule exhibits three diatropic ring-currents with 38 π-electrons in each, *i.e.*, it is a Type B expanded naphthalene. The hexacation $\mathbf{1}^{6+}$, a Type A expanded naphthalene, displays similar properties as **1** but with three 34π-electron rings. Both 34 and 38 are $4n + 2$ numbers so that **1** and $\mathbf{1}^{6+}$ with D_3 symmetry exhibit three Hückel-aromatic circuits similar as naphthalene, although naphthalene has fewer electrons with one 10π- and two 6π-electron circuits.

Now, how do the π-electron counts vary in these bicyclic compounds? When do they equal $6n + 2$? For Type A expanded naphthalenes the π-electron counts generally equal $4k + 4l + 4m + 2$, which when $k = l = m$ becomes $3\times4k + 2 = 6\times2k + 2$. With $n = 2k$ we get the π-electron count $6n + 2$. Thus, with three linkers of equal length the π-electron count of expanded naphthalene (macro)molecules coincides with the π-electron count of a truly 3D-aromatic molecule. This applies also for the Type B expanded naphthalenes as their π-electron counts simply are six additional π-electrons. Among **1** – **3** and $\mathbf{1}^{6+}$ it is therefore only **1** and $\mathbf{1}^{6+}$ that have total π-electron counts that can be summarized as $6n + 2$. Yet, will similar bicyclic cages as **1** and $\mathbf{1}^{6+}$ exhibit aromatic character also when $n \neq m$ and/or k? Indeed, if the tether lengths are just slightly different, *e.g.*, $k = l + 1 = m + 1$, then the π-electron count will not be a $6n + 2$ number, although, the structure should still allow for strong π-conjugation and Hückel-aromaticity in the three individual macrocyclic paths. Now, if these latter species are calculated

to be aromatic, that will disprove that **1** and $\mathbf{1}^{6+}$ are true 3D-aromatics; these two species are instead three times locally 2D Hückel-aromatic to equal extents.

But then, how to design π-conjugated (macrocyclic) cage molecules that are true 3D-aromatics? As it is the higher-order point groups that exhibit irreducible representations with triple (or higher) degeneracies, leading to species that possibly can be truly 3D-aromatic, a π-conjugated macrocycle that is truly 3D-aromatic must have (approximate) tetrahedral, octahedral or icosahedral symmetry. Furthermore, the local π-orbitals of the π-conjugated linkers must be oriented radially outward if they are to interact with the local p_π orbitals at the vertex atoms. We have also analyzed such tetrahedral and cubic species through computations (Figure 5A). These species would have radial orientations of their π-orbitals similar as charged fullerenes C_{60}^{10+} and C_{20}^{2+}, which have been explored computationally and found to follow Hirsch's $2(n + 1)^2$ rule as they are spherically aromatic.[27,48] Yet, Hirsch's rule has a limitation as it seems applicable only to species with 50 π-electrons or less.[49] A further caveat with regard to the cubic species is that each of the faces has $4m$ π-electrons ($m \neq n$), meaning that these can be Hückel-antiaromatic. Hence, the cubes can in theory be both globally 3D-aromatic and six-fold locally 2D-antiaromatic.

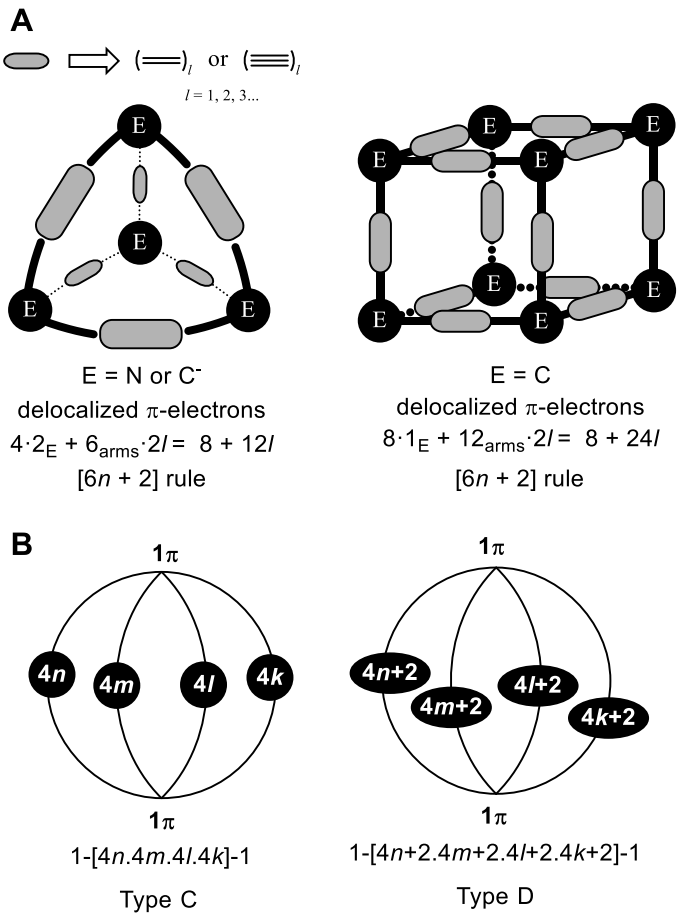

Figure 5. (A) Generalized design of potentially π-conjugated molecules which can be truly 3D-aromatic. (B) Generalized structures of expanded four-linker (Type C and Type D) polycyclic aromatic hydrocarbons with the number of π-electrons in the arms.

Another difference between true 3D-aromaticity and 2D-aromaticity-in-3D occurs for open-shell species which can adopt Baird-aromatic character. For a (macro)cyclic two-dimensional molecule which is Hückel-aromatic one can achieve a Baird-aromatic triplet state by either removal or addition of two electrons.[12] This is exemplified by the benzene dication and dianion for which there are derivatives shown experimentally to have either triplet multiplicity ground states or low-lying triplet states.[50-52] Similar to the benzene dication and dianion which are triplet state 2D-Baird-aromatic, true 3D-Baird-aromaticity will occur for the

trication and trianion as their π-electron occupancies allow for half-filled triply degenerate orbitals. Hence, true open-shell 3D-Baird-aromaticity will not occur for the triplet dication, and thus, it is noteworthy that $\mathbf{1}^{2+}$, which has a triplet ground state, has a NICS(0) value of -2.6 ppm,[35] suggesting some modest Baird-aromatic character. Yet, the triplet dication of a true 3D-aromatic species would have an electron configuration with four π-electrons in the triply degenerate HOMOs, an electron configuration that due to the Jahn-Teller effect should lead to a distortion away from the high-symmetry. Now, what is the electron count for Baird-aromaticity in a bicyclic macrocycle which is 2D-aromatic-in-3D? If one goes by simple π-electron counts, the quartet trication of both Type A and Type B expanded naphthalenes with $k = l = m$ can be Baird-aromatic as each linker will have $4k - 1$ π-electrons for Type A and $4k + 1$ π-electrons for Type B providing for *three* Baird-aromatic $4n$ circuits ($n = 2k$). Additionally, the triplet dication can be Baird-aromatic in one single cycle, as found by Wu and co-workers.[35] In contrast, for truly 3D-aromatic species it is *only* the trication in its quartet state that can exhibit Baird-aromaticity.

A further feature of 2D-aromaticity in a 3D structure is that it can be expanded to (hypothetical) macrocyclic structures with additional arms (Types C and D, Figure 5B). Here, it is noteworthy that a similar macrocyclic cage molecule with four tethers, yet with π-conjugated (aromatic) Ni-porphyrin units at its two poles, was recently reported by Wu and co-workers.[53] It was argued that the dication of this species unravels the relationship between 3D global aromaticity and 2D Hückel aromaticity. Yet, does it? When the molecules of Figure 5B have four linkers with equal numbers of π-electrons one has Gedanken-molecules which are 2D-aromatic-in-3D with six Hückel-aromatic $4n + 2$ cycles and with total π-electron counts of $8n + 2$; a π-electron count which is not in line with true 3D-aromaticity.

Computational analysis: Here we use quantum chemical calculations to probe the conceptual theories described above. We start by examining the electronic structure and aromaticity of naphthalene (**4**), puckered naphthalene (**5**) and the benzocyclooctatetraene dication (**6**) as 10π-electron bicyclic molecules, and connect these to the nonplanar dithiopheno-bridged octaphyrins **2** and **3** which have two long and one short bridges. Subsequently, we study bicyclic macrocycles with three bridges of (approximately) equal lengths whereby these compounds adopt cage-type structures. We especially analyze compounds that allow us to contest the presumption that **1** and $\mathbf{1}^{6+}$ are true 3D-aromatics that follow the $6n + 2$ and $2(n + 1)^2$ rules. Should they instead be categorized as 2D-aromatics with 3D structures? Towards the end, we explore tetrahedral and cubic π-conjugated compounds (Figure 5A) with potentials to be true 3D-aromatics. Throughout, we focus on effects in the closed-shell electronic ground state but also analyze high-spin states of the doubly and triply oxidized species and their potential Baird-type aromaticity.

At this point, it should be stressed that the study is qualitative rather than quantitative as we explore type of aromaticity, not the quantitative degree of aromaticity. For that reason, we utilize primarily a functional (B3LYP)[54-56] which is known to exaggerate aromaticity in macrocycles when compared to long-range corrected functionals (*e.g.*, CAM-B3LYP)[57] which are recommended for such molecules[58] and for aromatic compounds in general.[59] Calculations with CAM-B3LYP are performed on selected species. Aromaticity analyses are performed through the electron density of delocalized bond (EDDB) function,[60,61] nucleus independent chemical shifts (NICS),[62-65] anisotropy of induced current density (ACID),[66] as well as current densities calculated with GIMIC.[67] EDDB reveals that benzene, being a reference for an aromatic species, has 5.3 delocalized π-electrons, *i.e.*, 88% of the six π-electrons participate in cyclic delocalization over the hexagon. Conversely, in cyclobutadiene at its rectangular (D_{2h}) structure and cyclooctatetraene at its planar D_{4h} symmetric structure the extent of π-electron

delocalization is 0% and 2.5%, respectively. This clarifies the wide span in the electron delocalization between aromatic and antiaromatic annulenes.

Nonplanar dithiopheno-bridged octaphyrins as expanded naphthalenes: Naphthalene is planar, D_{2h} symmetric and exhibits three Hückel-aromatic cycles (Figure 3); two with six and one with ten π-electrons. This becomes apparent through electronic aromaticity indices. For example, EDDB reveals delocalization through both the perimeter and the central CC bond, and as the electronic structure is a superposition of the π-dectet and the two π-sextets resonance forms, the EDDB-based percentage effectiveness of cyclic delocalization of π-electrons in each cycle is similar.[47] In contrast, and as noted above, magnetic indices give an obscured picture since the induced ring currents from the two hexagons cancel each other perfectly in the central CC bond.[42] This is also clear from the current densities obtained with GIMIC as the average current strength in the perimeter bonds is ~13 nAT^{-1} (diatropic) while the current strength in the central CC bond is nil. Yet, when gradually distorting one of the hexagons leading to a puckered C_s symmetric structure (**5**, Figure 6A) the ring current in the puckered hexagon is attenuated whereby the two 6π-electron ring currents do not cancel anymore and a current density in the inter-ring CC bond emerges (for current densities of gradually more distorted naphthalenes see Tables S1 and S3). One can also see that the π-electron delocalization is very attenuated in the puckered hexagon while it is enhanced in the planar hexagon (Figure 6A).

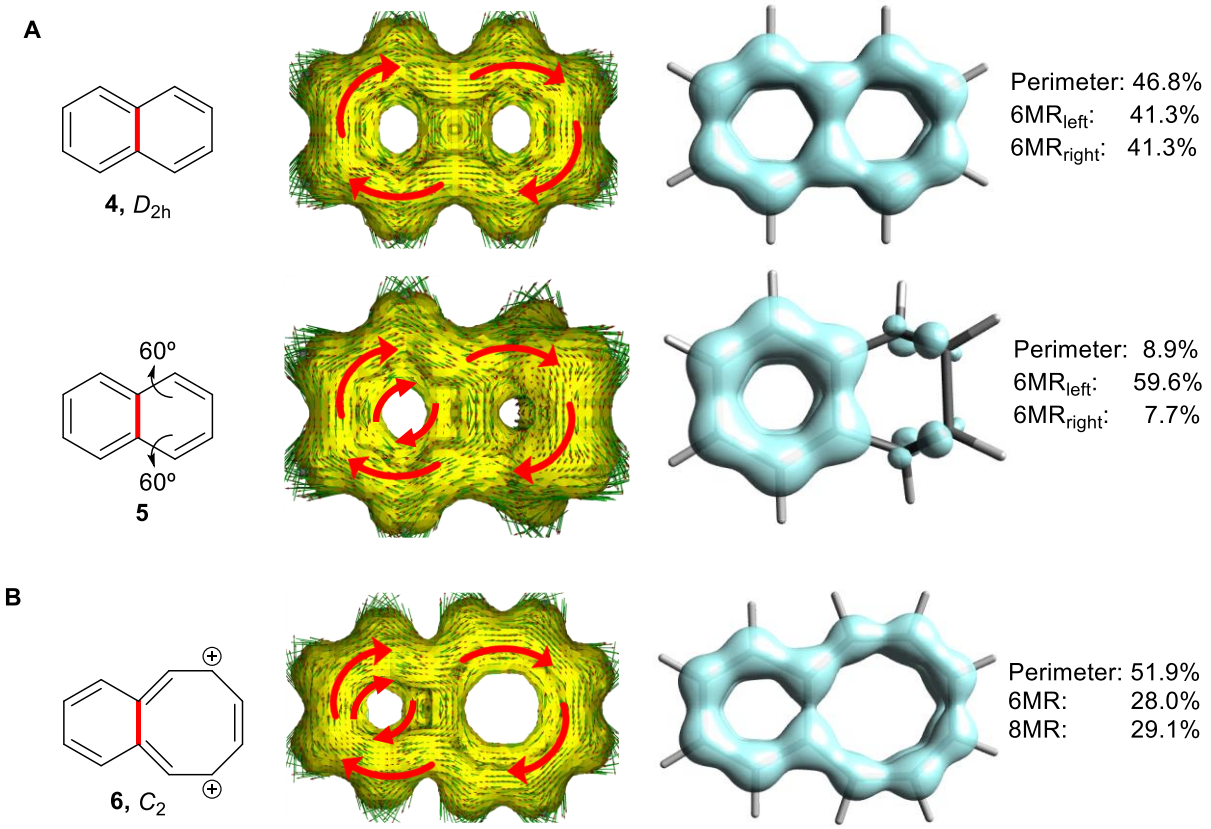

Figure 6: (A) Naphthalene in its planar (**4**) and puckered (**5**) structures and the corresponding ACID and EDDB plots. (B) Molecular structure and symmetry of benzoCOT dication (**6**). *n*MR = *n*-membered ring. For full-scale images of the ACID plots for **4**, **5** and **6** as well as naphthalene at other distortion angles of **4**, see Figures S1 and S2.

Yet, it is also possible to achieve a differentiation in the 6π-electron currents, and a current density in the inter-ring CC bond, by going to the nearly planar benzocyclooctatetraene dication (**6**) (Figure 6B). For **6**, a NICS-*XY* scan also shows that the local 6π-electron aromaticity in the hexagon dominates over that in the octagon whereby the resulting current density in the central CC bond is 4.7 nAT^{-1}. Clearly, a structural differentiation between the two 6π-electron cycles, achieved either by distortion or altered ring size, provides for a differentiation in the ring currents of the two cycles, leading to an imperfect cancellation of the currents in the inter-ring CC bond. In **2** and **3**, the dissimilarities between the two 26π-electron

cycles come about because of the orientation of the dithienothiophene (DTT) bridge which leads to a better π-conjugation with one half of the octaphyrin than with the other half, reflected in C-C-C-C dihedral angles to the DTT bridge which are 7 and 33º, respectively. This provides a better electron delocalization in one 26π-electron cycle than in the other (41.7 *vs*. 35.6%), although the best delocalization is along the perimeter (42.5%).

Now, can one instead turn the dithienothiophene-bridged octaphyrins into compounds with similar features as planar naphthalene; that is, can they be turned into symmetric (and near-planar) molecules with no current densities on the central bridge? The [34]octaphyrin, *i.e.*, **2** without the DTT bridge, adopts a modestly helical structure 0.2 kcal/mol lower in energy than a planar C_{2v} symmetric structure (a first-order saddle point). However, the DTT bridge is too long by ~0.9 Å to fit into an [34]octaphyrin (see Figure S3), and its incorporation leads to the strongly puckered compound. Indeed, a planar C_{2v} symmetric structure is a higher-order saddle point 87.0 kcal/mol above the minimum. The importance of the nonplanarity for the observations made by Kim and co-workers becomes obvious through an ACID plot of the planar C_{2v} structure because now the two 26π-electron ring currents are of similar weights and cancel on the bridge whereas the current through the perimeter remains (Figure S4). In the planar structure of **2** there is a slight reduction in the difference in the extent of delocalization between the two 26π-electron cycles (34 *vs.* 39%). Hence, it is the non-equivalence of the two 26π-electron resonance structures of **2** and **3** effectuated through the non-planar structures and the larger C-C-C-C dihedrals within one macrocyclic path than on the other that leads to the observation of two strong ring currents with, respectively, 34 and 26 π-electrons and one with weakened strength. It is apparent that these macrocycles resemble distorted naphthalene.

To achieve a planar octaphyrin-based macrobicyclic species, the DTT bridge was replaced by a shorter butadiyne bridge and the two pyrrole rings adjacent to the bridgehead C

atoms were linked pairwise via methylene bridges. This leads to the D_{2h} symmetric **7**, a compound that displays only a perimetric ring current with current densities in the range 23 – 33 nAT^{-1} (Figure 7). To achieve a differentiation between the two 22π-electron macromonocycles in a near-planar macrobicycle, we replaced two CH moieties on one side by two SiH moieties, leading to **8**. According to ACID, two clockwise ring-currents can be detected for this species; one over the perimeter and one over one of the 22π-electron cycles (Figure 7B). As seen visually, the 22π-electron cycle with the stronger ring current is the ring with CH units. The NICS-*XY* scans also show that the aromatic character of one of the two macromonocycles decreases when going from **7** to **8**. Hence, there is an imperfect cancellation of the two 22π-electron ring-currents in the butadiyne-bridge of **8**, analogous to the situation in **6** (Figure 6). GIMIC reveals current strengths of 11.7 - 14.4 nAT^{-1} at this bridge. Interestingly, EDDB reveals that the extent of delocalization in the two macromonocycles of **8** are, respectively, larger and smaller than in the two equivalent macromonocycles of **7** (Figure 7C).

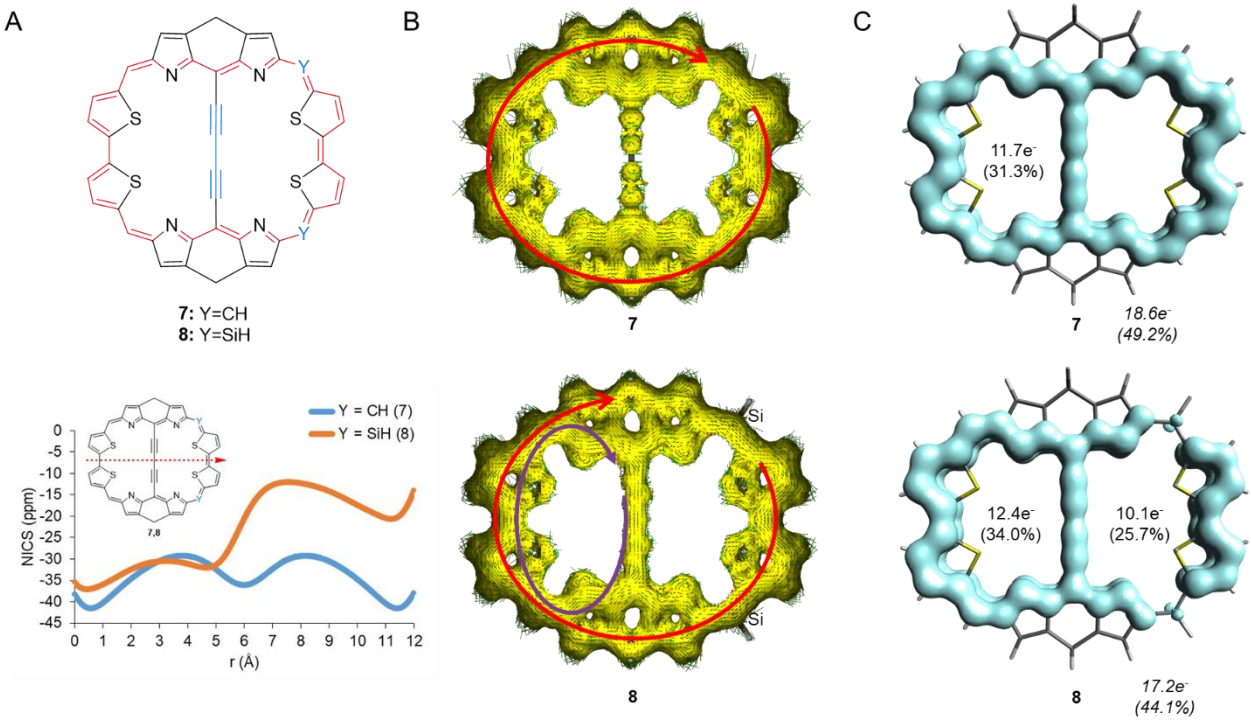

Figure 7: (A) Expanded naphthalenes modelled from **2** and NICS-*XY* scans for the expanded naphthalenes **7** (blue) and **8** (dark orange), (B) ACID plots with the induced current densities of **7** and **8**, and (C) EDDB plots of **7** and **8**. For full-scale images of the ACID plots, see Figures S5 and S6.

Furthermore, Kim and co-workers argued that the triplet state of the dication of **2** ($^{3}\mathbf{2}^{2+}$) can be described as having one 33π-electron cycle in the perimeter and one 25π-electron circuit in one of the individual macrocycles.[35] Based on the findings above, we instead reason that $^{3}\mathbf{2}^{2+}$ should be described as a distorted expanded naphthalene dication which is triplet state 2D-Baird-aromatic in the conventional sense. The naphthalene dication in its triplet state ($^{3}\mathbf{4}^{2+}$) is described by three Baird-aromatic resonance structures; two with 4π-electron circuits in either of the hexagons and one with an 8π-electron perimeter (Figure 8A). When this triplet state naphthalene dication is distorted ($^{3}\mathbf{5}^{2+}$) the two 4π-electron cycles will become inequivalent; one remains unaltered while the other is weakened. Similarly, $^{3}\mathbf{2}^{2+}$ should be described primarily by two 4*n*π-electron Baird-aromatic resonance structures; one with a 32 π-electron perimetric circuit and one with a 24π-electron circuit in one of the two macromonocycles. When $^{3}\mathbf{5}^{2+}$, $^{3}\mathbf{2}^{2+}$ and $^{3}\mathbf{8}^{2+}$ are explored with EDDB it becomes clear that the π-electron delocalization is attenuated by the puckering as well as by the C-to-Si replacements.

Next, when the middle tether of **2** and **3** is extended so that the three tethers become equal, the expanded naphthalenes turn into cage (macro)molecules such as **1**.

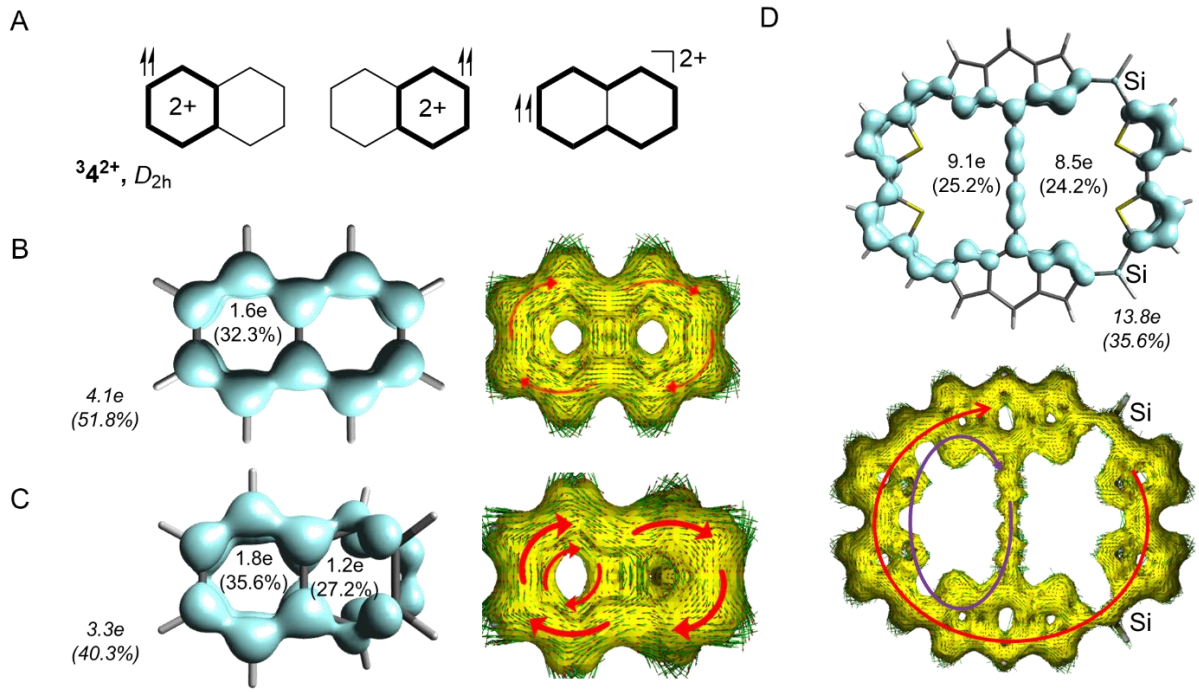

Figure 8: (A) Schematic resonance structures of available 4*n* π-electron circuits in naphthalene dications. The triplet state naphthalene dication in the (B) planar (^{3}**4**$^{2+}$) and (C) distorted (^{3}**5**$^{2+}$) structures, both ACID and EDDB plots, and (D) EDDB and ACID plots of **8**$^{2+}$. For full-scale images of the ACID plots for ^{3}**4**$^{2+}$, **8**$^{2+}$ and different distortions of ^{3}**4**$^{2+}$, see Figures S7 - S9.

On the aromaticity of fully π-conjugated cage macrocycles: Despite the obvious three-dimensional structures of **1** and **1**$^{6+}$, and that the globally aromatic characters of the molecular cages when D_3 symmetric are apparent, they are not truly 3D-aromatic. Instead their aromaticity can be understood in terms of the conventional Hückel-aromaticity of polycyclic aromatic hydrocarbons, which in most cases is two-dimensional. We therefore label these compounds as 2D-aromatic-in-3D. Also **1** and **1**$^{6+}$ can be viewed as expanded naphthalenes (Figure 4B-C), now where the middle tether has been elongated so that the π-electron counts in the three macrocyclic paths become equal. As noted above, the D_3 symmetry does not provide the compounds with the required orbital topology for true 3D-aromaticity. Furthermore, in neutral **1**, the dihedral angles between the tethers at the bridgehead atoms (δ_1, δ_2 and δ_3, Figure

9) are 26°, 46° and 48°, which reveals that only one of the three cyclic paths is significantly π-conjugated over the two bridgeheads as the π-orbital overlap between two p_π AOs scales as cosθ with θ being the angle between the two AOs.[68] Yet, with the other dihedral angles in that (aromatic) cycle being 154 - 171°, its π-conjugation is also attenuated. It was earlier reported that when D_3 symmetric there is an equal aromaticity in the three rings, giving **1** an aromatic character that (seemingly) extends over the complete molecule. However, as concluded above, the equal extent of aromaticity in the three rings is a necessary result of the symmetry-adapted electronic structure and is not due to 3D aromaticity. Furthermore, the D_3 symmetric structure of $\mathbf{1}^{6+}$ maximizes the possibility to mutually separate six positive charges. Thus, its enhanced aromatic character is a by-product of charge repulsion, and it has been observed earlier that oxidized macrocycles often have enhanced aromatic character when compared to the corresponding neutral macrocycles.[69] In this context, it is notable that $\mathbf{1}^{6+}$ has $\delta_1 = \delta_2 = \delta_3 = 41°$, and with two such dihedrals in each macrocyclic ring the π-conjugation will still be attenuated since $[\cos(41°)]^2 = 0.57$.

As $\mathbf{1}^{6+}$ has a π-electron count of 50, Casado and Martín described it as spherically aromatic fulfilling Hirsch's $2(n + 1)^2$ rule with $n = 4$.[36] Here, it is noteworthy that Wu and co-workers very recently concluded that a similar C_2 symmetric cage-type macrocycle with four tethers does not follow this rule.[53] Now, to probe if $\mathbf{1}^{6+}$ complies with Hirsch's rule, or if the π-electron count is merely coincidential, we analyzed the next larger analogue of $\mathbf{1}^{6+}$, leading to $\mathbf{11}^{6+}$ with five instead of four thiopheno rings in each tether. According to EDDB this hexacation exhibits slightly more π-electron delocalization than $\mathbf{1}^{6+}$ (60.0% in $\mathbf{11}^{6+}$ and 59.5% in $\mathbf{1}^{6+}$) and would be equally aromatic. Yet, $\mathbf{11}^{6+}$ has 62 π-electrons, a number which is not a $2(n + 1)^2$ number (the next is 72 when $n = 5$). Instead, the slightly enhanced π-electron delocalization of $\mathbf{11}^{6+}$ seems to be a result of the longer tethers which allow for better π-orbital

overlap at the bridgehead C atoms because the δ_1 - δ_3 values are lower in $\mathbf{11}^{6+}$ than in $\mathbf{1}^{6+}$ (36° *vs.* 41°). Thus, the reason that the π-electron count of $\mathbf{1}^{6+}$ is a $2(n + 1)^2$ number is coincidental.

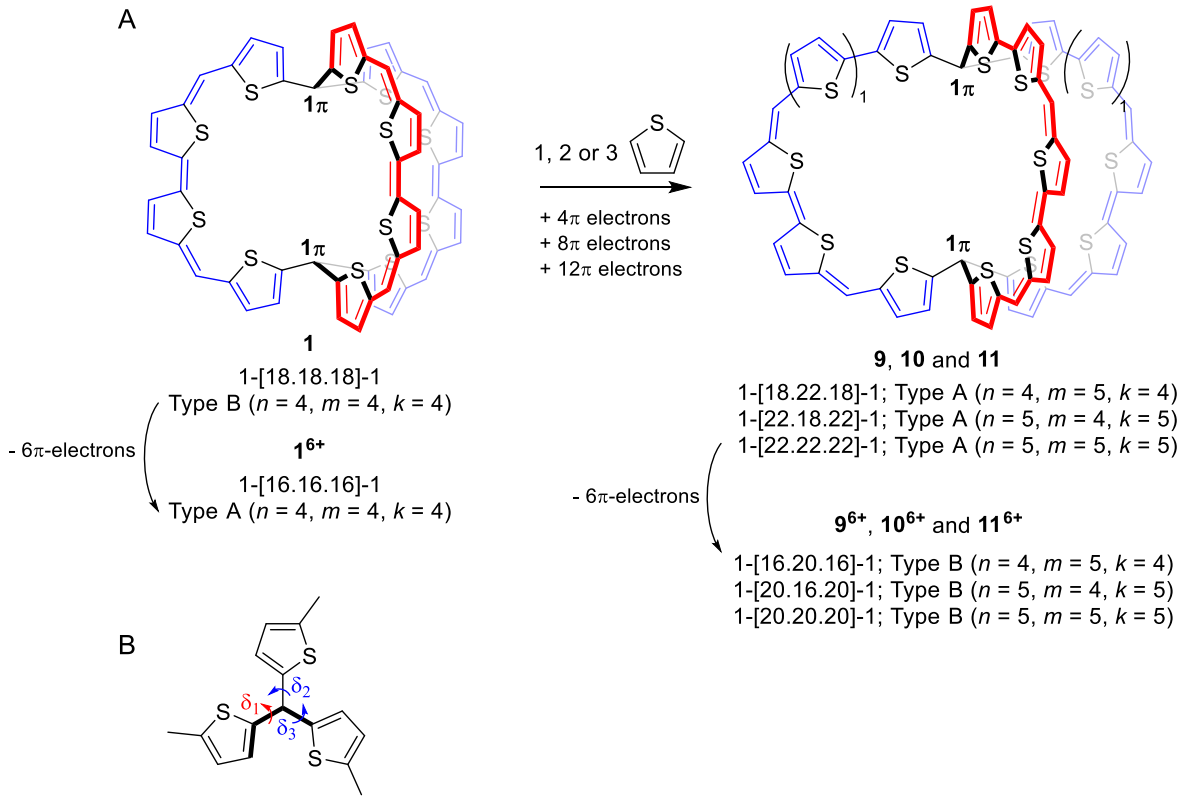

Figure 9. (A) Molecular cage **1** inserting one more thiopheno ring in each tether leading to species with total π-electron counts of 60 (**9**), 64 (**10**) and 68 π-electrons (**11**) and their hexacations. (B) Relevant dihedral angles (δ) in the molecular cages.

The π-electron count of $\mathbf{11}^{6+}$ is not a $2(n + 1)^2$ number but it is a $6n + 2$ number. Yet, also this π-electron count does not correspond to true 3D-aromaticity since a π-electron count of $6n + 2$ results coincidentally for a bicyclic molecule with three equal tethers, as described in the theory section above. To confirm this, we asked if cage macrocycles where one linker has four more π-electrons (or four less) than the other two linkers are similarly aromatic as $\mathbf{1}^{6+}$ and $\mathbf{11}^{6+}$? We tested this through $\mathbf{9}^{6+}$ and $\mathbf{10}^{6+}$ (Figure 9) with total π-electron counts of 54 and 58, *i.e.*, counts that are not $6n + 2$ numbers. We now find that the extent of π-electron delocalization

according to EDDB is similar in the four hexacations (Figure 10), revealing that it is not the specific $6n + 2$ π-electron count in $\mathbf{1}^{6+}$ and $\mathbf{11}^{6+}$ which leads to the high delocalization in these species. Instead, all four species ($\mathbf{1}^{6+}$, $\mathbf{9}^{6+}$, $\mathbf{10}^{6+}$ and $\mathbf{11}^{6+}$) are 2D-aromatic in a 3D structure, which should be the reason for their high electron delocalizations. Notably, similar results were calculated with CAM-B3LYP as with B3LYP (see the Table S4). Furthermore, by starting at **11** and shortening one of the tethers by either two or three thiopheno rings we arrive at cage compounds **12** and **13** where the extent of delocalization starts to differ between the macrocyclic paths (see Table S4). In **12** the electron delocalization in one circuit reaches 52% while it is 41 - 42% in the other two, and in **13** these numbers are 54% and 38%, respectively. This is even a stronger differentiation than seen in **2**.

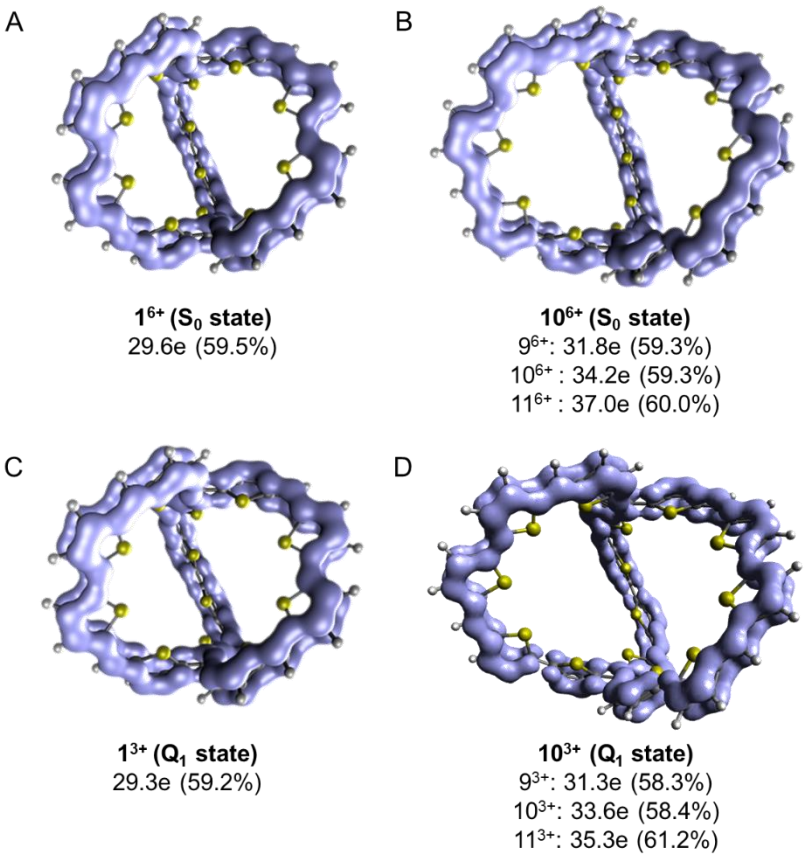

Figure 10: EDDB results of (A) $\mathbf{1}^{6+}$ and (B) $\mathbf{9}^{6+}$, $\mathbf{10}^{6+}$ (EDDB plot shown) and $\mathbf{11}^{6+}$ in their closed-shell singlet ground states, and (C) $\mathbf{1}^{3+}$ and (D) $\mathbf{9}^{3+}$, $\mathbf{10}^{3+}$ (EDDB plot shown) and $\mathbf{11}^{3+}$

in their lowest open-shell quartet states. For the percentage delocalized electrons per cycle, see Table S4 in the SI.

Finally, it was earlier argued that the dication of **1** in its triplet state ($^{3}\mathbf{1}^{2+}$) is Baird-aromatic in one of the cycles since it has a NICS(0) value of -2.6 ppm,[35] a value that suggests a modest Baird-aromaticity (if any). Following the argumentation in the section on qualitative theory we tested if Baird-aromaticity is also achieved in the quartet state of the trication, and find that $^{4}\mathbf{1}^{3+}$ is D_3 symmetric at its global minimum having an electron delocalization of 59% (EDDB), and a similar delocalization is found in the triplet dication ($^{3}\mathbf{1}^{2+}$) (62%). Furthermore, as D_3 symmetry does not provide for triple degeneracy one may ask how the half-filled MOs which support the high symmetry of $^{4}\mathbf{1}^{3+}$ look like? An inspection of the three highest α-SOMOs reveals a pair of doubly degenerate MOs and a non-degenerate totally symmetric MO (see Figure S11), leading to an orbital occupancy of the quartet trication that complies with D_3 symmetry. This leads to a symmetric distribution of the unpaired electrons and explains why the trication in its quartet state can keep D_3 symmetry despite that there are no triply degenerate sets of orbitals.

Search for truly 3D-aromatic π-conjugated cage molecules: Now, can one design π-conjugated molecules which are true 3D-aromatics? Both the $6n + 2$ electron count and the orbital topology requirements must be fulfilled in such molecules. They should also exhibit extensive electron delocalization in radially oriented π-orbitals and it should be larger than the delocalization for analogous species with other electron counts than $6n + 2$. In the theory section, we outlined the design of tetrahedral and cubic π-conjugated molecules which may be true 3D-aromatics (see Figure 5A). The design starts at the tetrahedral E_4^{4-} and cubic E_8 species, and we insert, respectively, six and twelve π-conjugated linkers between the vertex atoms in the two structures. Carbon atoms were chosen at the vertices as they provide for stronger π-

conjugation than the heavier Group 14 elements which are found in tetrahedral Zintl ions earlier labelled as 3D-aromatic.[28] For the tetrahedral species, we also considered N atoms at the vertices but they lowered the π-electron delocalization (see Figure S12). With four anionic sp^3 hybridized C atoms (tetrahedral species) or eight neutral sp^2 hybridized C atoms (cubic species) we formally have, in both cases, eight radially oriented electrons at the vertices which can conjugate with the electrons in the radial π-orbitals of the linkers. Both polyene and polyyne linkers were considered, yet, we start with the rigid polyyne linkers butadiynyl, hexatriynyl or octatetraynyl which contribute with four, six or eight electrons to radially oriented π-orbital frameworks.

The $C_4(C_q)_6^{4-}$ species (q = 4 (**14**), 6 (**15**) or 8 (**16**)) are T_d symmetric and the π-electron delocalization increases with linker length from 14% in **14** to 24% in **16**. Thus, the delocalization in the radial π-orbital framework of **16**, which is bent, is slightly lower than that of planar furan (27%) but modest when compared to that of pyrrole (48%). When calculated with CAM-B3LYP the delocalization in **16** decreases to 15%, although the molecule still keeps its tetrahedral structure. Interestingly, for the cubes $C_8(C_4)_{12}$ (**17**) and $C_8(C_6)_{12}$ (**18**) the extent of delocalization of the radial π-electrons are higher at 43% and 42%, respectively. Based on the CC bond lengths within the hexatriyne segments of **18** (1.229 – 1.330 Å) as compared to those of 1,3,5-hexatriyne (1.209 - 1.356 Å), it is further clear that there is some degree of bond length equalization in **18** indicative of enhanced delocalization.

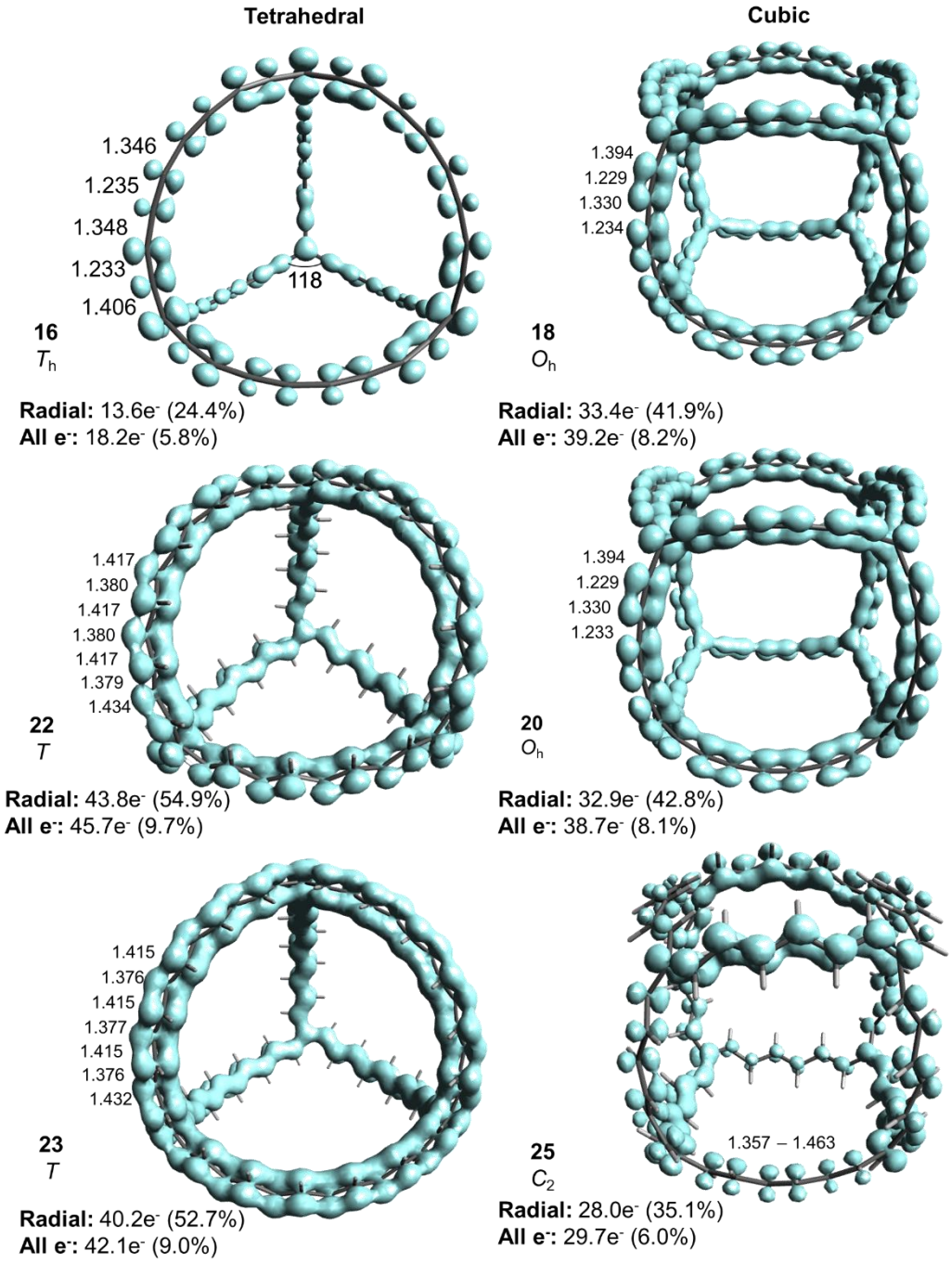

Figure 11. Structures displaying the bond lengths as well as the EDDB plots of $C_4(C_8)_6^{4-}$ (**16**), $C_4(C_{12}H_{12})_6^{4-}$ (**22**), $C_4(C_{12}H_{12})_6^{-}$ (**23**) (quartet state), $C_8(C_6)_{12}$ (**18**), $C_8(C_6)_{12}^{3+}$ (quartet state, **20**), $C_8(C_6H_6)_{12}$ (**25**). Distances in Å and angles in deg. The EDDB results based on all radial π-MOs and on all MOs are both given. Essential molecular orbitals found in Figures S14 and S15 of the SI.

Zintl ions such as Si_4^{4-} and white phosphorous P_4 have earlier been concluded to be 3D-aromatic based on NICS(0) values computed in the tetrahedron centers.[28] Yet, as the electron delocalization decreases with shorter tethers, it should be the lowest in the E_4^{4-} species. Indeed, according to EDDB these species are devoid of electron delocalization in the π-orbitals (0.5% in Si_4^{4-} and P_4), and also when all orbitals are included (0.2% in both cases). Accordingly, they should not be labelled as true 3D-aromatics, and current density plots reveal that the highly negative NICS values observed earlier[28] stem from local diatropic circulations around the lone-pairs (see section B in the Supporting Information). This is in contrast to *closo*-boranes which exhibit extensive delocalization (see section C of the Supporting Information) and certain smaller charged fullerenes.[21,49]

As **16**, **17** and **18** formally have $6n + 2$ π-electrons that can be assigned to radially oriented π-MOs, and since they exhibit weak electron delocalization, one may ask if the highest occupied MO levels all are triply degenerate and radially oriented? A visual inspection shows that this is not the case for **16** but for **17** and **18** (Figure 12). Although HOMO of **16** is triply degenerate and described purely by radially oriented p_π AOs, HOMO-1 and HOMO-2 are nondegenerate, and HOMO-3 is a mix of radially and in-plane oriented p_π. Thus, **16** should *not* be labelled as a 3D-aromatic that fulfills the $6n + 2$ rule, and the same applies to **14** and **15**. Clearly, as the local bond orbitals with either in-plane or radial orientations mix for the tetrahedra, the polyyne linkers are not suitable for construction of tetrahedral π-conjugated 3D-aromatics. In contrast, in the cubic **18**, combinations of radially and in-plane oriented p_π AOs are only found in orbitals of very low energy (HOMO-59 and HOMO-67).

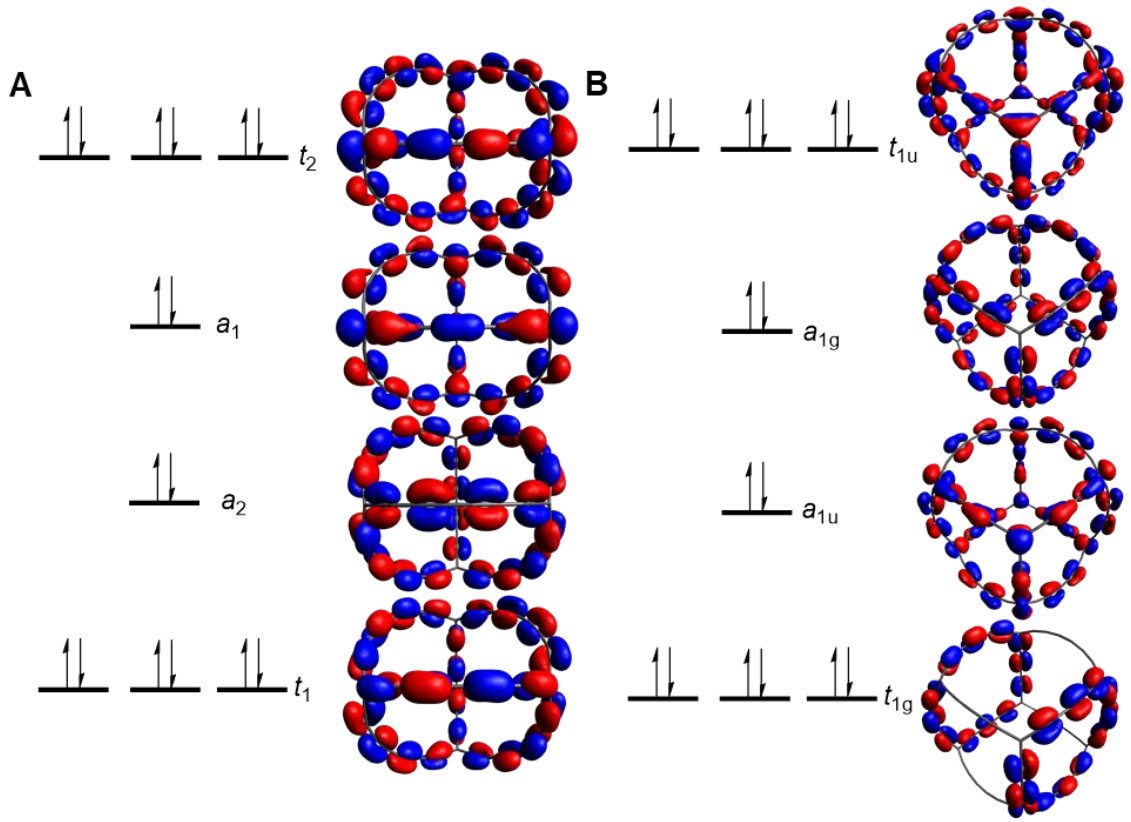

Figure 12: The highest few occupied molecular orbitals (A) $C_4(C_8)_6^{4-}$ (**16**) (T_h symmetric) and (B) $C_8(C_6)_6$ (**18**) (O_h symmetric) at the optimal B3LYP/6-311G(d,p) geometries. The symmetry of the orbitals is also specified. For full-image orbital plots, see Figures S14 and S15.

Instead of polyyne linkers in the tetrahedra, we turned to all-*E*-polyenes in their all-s-*trans* conformations, leading to the *T* symmetric $C_4(C_{10}H_{10})_6^{4-}$ (**21**) and $C_4(C_{12}H_{12})_6^{4-}$ (**22**). These two compounds only have radially oriented π-orbitals. Moreover, EDDB reveals that **21** and **22** have significantly stronger radial π-electron delocalization (41 and 55%, respectively) compared to those with polyyne linkers. Interestingly, for the cubic species such as $C_8(C_4H_4)_8$ (**24**) and $C_8(C_6H_6)_8$ (**25**) the polyene linkers lead to structures which are distorted (C_2 symmetric) with weaker delocalization (35%) than found for the corresponding polyyne-linked species (Figure 11). Furthermore, they exhibit significant bond length alternations as seen for **25**.

Now, if the polyene-linked C_4^{4-} and the polyyne-linked C_8 species are truly 3D aromatic then similar compounds but with electron counts that differ from $6n + 2$ should be nonaromatic and exhibit lower electron delocalization. Yet, this is not the case for neither of the species. Only a minutely decreased delocalization is calculated when going from the tetrahedral **22** to $C_4(C_{12}H_{12})_4(C_{10}H_{10})_2^{4-}$ (**26**) (55% in **22** and 54% in **26**). The same is observed for the cubic species, and sometimes the delocalization is even minutely increased (*e.g.*, 41% in **18** and 42% in $C_8(C_4)_8(C_6)_4$ (**27**)).

Finally, we explored if 3D-Baird-aromatic structures can be reached by removal of three electrons from **22** leading to quartet state $^4C_4(C_{12}H_{12})_6^-$ (**23**), and from **17** and **18** to the quartet state $^4C_8(C_4)_{12}^{3+}$ (**19**) and $^4C_8(C_6)_{12}^{3+}$ (**20**) (Figure 11E). These three species are minima and adopt, respectively, *T* and O_h symmetric structures, while the triplet dications distort away from the high symmetries due to Jahn-Teller distortions, as predicted above. Furthermore, EDDB reveals that **23** has a very similar extent of delocalization (53%) as the closed-shell **22** (55%). To check if **23** has some true 3D-Baird-aromatic character we examined two similar compounds, $C_4(C_{12}H_{12})_4(C_{10}H_{10})_2^-$ (**28**) and $C_4(C_{12}H_{12})_2(C_{10}H_{10})_4^-$ (**29**), for which the electron counts differ from $6n + 2$. Yet, similar extents of delocalization (53% for both) as for **23** were calculated. Next, in case of the tricationic cubes in their quartet state (**20 - 22**), the delocalization is very similar to their respective neutral analogues in the singlet ground state. In cubes that do not follow the rule (such as $C_8(C_4)_4(C_6)_8^{3+}$ (**30**) and $C_8(C_6)_4(C_4)_8^{3+}$ (**31**)), the delocalization remains almost unchanged (42% and 41%, respectively). Consequently, it becomes clear that also the potential 3D-Baird-aromatic character of **23** in its quartet state is unlikely.

Taken together, we have revealed the sincere difficulty to design π-conjugated molecules (neutral or charged) which are truly 3D-aromatic.

Conclusions

Using qualitative theory combined with quantum chemical calculations, we came up with key points that help to discern between regular 2D-aromaticity, albeit in a 3D molecular structure, and true 3D-aromaticity in three-dimensional π-conjugated (cage) (macro)molecules. Our study revealed that compounds $\mathbf{1}^{6+}$ and **2** (and **3**) should not be labelled as, respectively, 3D aromatic and bicycloaromatic. The basic prerequisite for true 3D-aromaticity, besides $6n + 2$ π-electron counts and high π-electron delocalization, is a highly symmetric structure with at least triply degenerate MOs, features that do not exist in $\mathbf{1}^{6+}$. Yet, there are also clear limitations for tetrahedral and cubic cage compounds that formally fulfill the 3D-aromaticity requirements because there are negligible differences in electron delocalization between these cage compounds and near-tetrahedral or near-cubic compounds that have π-electron counts that deviate from $6n + 2$. Hence, there seems to be a size limitation for true 3D-aromaticity, similar as has been observed earlier for spherical aromaticity.[49]

Likewise, the main features of bicycloaromatic species do not exist in **2** and **3**. Instead, we find that the three macrocyclic molecules **1** – **3** and $\mathbf{1}^{6+}$ are better described as 2D-aromatic-in-3D since their aromatic character originates from the presence of various 2D Hückel-aromatic circuits in three-dimensional molecular scaffolds. In that regard, we showed that not only is there a direct connection between PAHs (*e.g.*, naphthalene) and $\mathbf{1}^{6+}$ and **2** (as well as **3**), but also a connection between the three macrocycles. It becomes clear that they all can be described as expanded naphthalenes.

Building on the findings we further attempted to design true 3D aromatic species and identified caveats that make their design difficult. First, the difficulty in getting a sufficient number of triply degenerate MOs with only radial orientation. Ideally, in a highly symmetric structure, the 3D aromatic character would only come from radial π-MOs, whereas if such orbitals exist in combination with other MO types, then the molecule is not a true 3D aromatic.

A second weakness is the fact that the extent of electron delocalization in species that fulfill the $6n + 2$ electron count barely differs from those that do not fulfill this count.

In conclusion, no truly 3D-aromatic π-conjugated molecule has to our knowledge so far been described in experiments. At this point we want to stress that, although we bring a different rationalization of the aromaticity in **1** – **3** and $\mathbf{1}^{6+}$ than provided earlier,[35-37] it is truly important that new compounds that stretch and provoke our understanding of chemical bonding phenomena are designed and analyzed. Healthy discussions on their chemical bonding brings chemistry forward as a science.

Computational methods

All geometry optimizations were performed with Gaussian 16[70] at the B3LYP/6-311G(d,p) level,[54-56] although a selected species were also calculated with CAM-B3LYP.[57] Aromaticity was evaluated in terms of electronic and magnetic indicators at the same level of theory. The electronic delocalization was evaluated by the electron density of delocalization bond ($EDDB_H$),[60,61] and magnetic properties were assessed using the nucleus-independent chemical shift (NICS),[62-63] anisotropy of the induced current density (ACID)[66] plots and gauge-including magnetically induced currents (GIMIC).[67] Regarding $EDDB_H$ computations, NBO 3.1[71] and Multiwfn have been employed, where the former together with Avogadro 1.2[72,73] was used to obtaining $EDDB_H$ surfaces. NICS-*XY* scans were performed using the Aroma package[74] and ACID plots were produced using AICD 2.0.0 program.[75,76]

Acknowledgements

First, we are grateful to Prof. Per-Ola Norrby for discussions at the early stage of the project reported herein. O.E.B. is grateful to the Wenner-Gren Foundations for a postdoctoral fellowship (UPD 2018-0305), and H.O., K.J. and R.A. acknowledge the Swedish Research

Council for financial support (grants 2015-04538 and 2019-05618). M.S. is grateful for the financial support from the Spanish MICINN (project PID2020-113711GB-I00) and the Catalan DIUE (project 2017SGR39). D. W. S. acknowledges the financial support by the European Union's Framework Programme for Research and Innovation Horizon 2020 (2014–2020) under the Marie Skłodowska-Curie Grant Agreement No. 797335 "MulArEffect". The computations were enabled by resources provided by the Swedish National Infrastructure for Computing (SNIC) at the National Supercomputer Center (NSC), Linköping, partially funded by the Swedish Research Council through grants 2015-04538 and 2019-05618.

References

1 Yoon, Z. S.; Osuka, A.; Kim, D. Möbius Aromaticity and Antiaromaticity in Expanded Porphyrins. *Nat. Chem.* **2009**, *1*, 113–122.

2 Zhu, C.; Luo, M.; Zhu, Q.; Schleyer, P. v. R; Wu, J. I-C.; Lu, X.; Xia, H. Planar Möbius Aromatic Pentalenes Incorporating 16 and 18 Valence Electron Osmiums. *Nat. Commun.* **2014**, 5, 3265.

3 Tanaka, T.; Osuka, A. Chemistry of *meso*-Aryl-Substituted Expanded Porphyrins: Aromaticity and Molecular Twist, *Chem. Rev.* **2017**, *117*, 2584-2640.

4 Szyszko, B.; Białek, M. J.; Pacholska-Dudziak, E.; Latos-Grażyński, L. Flexible Porphyrinoids, *Chem. Rev.* **2017**, *117*, 2839-2909.

5 Cheung, L. F.; Kocheril, G. S.; Czekner, J.; Wang, L.-S. Observation of Möbius Aromatic Planar Metallaborocycles, *J. Am. Chem. Soc.* **2020**, *142*, 3356-3360.

6 Szczepanik, D. W., Solà, M. Electron Delocalization in Planar Metallacycles: Hückel or Möbius Aromatic?, *ChemistryOpen* **2019**, *8*, 219-227.

7 Popov, I. A.; Pan, F.-X.; You, X.-R.; Li, L.-J.; Matito, E.; Liu, C.; Zhai, H.-J.; Sun, Z.-M.; Boldyrev, A. I. Peculiar All-Metal σ-Aromaticity of the $[Au_2Sb_{16}]^{4-}$ Anion in the

Solid State. *Angew. Chem. Int. Ed.* **2016**, *55*, 15344–15346.

8 Wan, P.; Krogh, E. Evidence for the Generation of Aromatic Cationic Systems in the Excited State. Photochemical Solvolysis of Fluoren-9-ol, *Chem. Commun.*, **1985**, 1207–1208.

9 Shukla, D.; Wan, P. Evidence for a Planar Cyclically Conjugated 8π System in the Excited State: Large Stokes Shift Observed for Dibenz[*b*,*f*]oxepin Fluorescence, *J. Am. Chem. Soc.* **1993**, *115*, 2990-2991.

10 Ottosson, H.; Kilså, K.; Chajara, K.; Piqueras, M. C.; Crespo, R.; Kato, H.; Muthas, D. Scope and Limitations of Baird's Theory on Triplet State Aromaticity: Application to the Tuning of Singlet–Triplet Energy Gaps in Fulvenes. *Chem. Eur. J.* **2007**, *13*, 6998–7005.

11 Rosenberg M.: Ottosson H.; Kilså K. Influence of Excited State Aromaticity in the Lowest Excited Singlet States of Fulvene Derivatives, *Phys. Chem. Chem. Phys.* **2011**, *13*, 12912-12919.

12 Sung, Y. M.; Yoon, M.-C.; Lim, J. M.; Rath, H.; Naoda, K.; Osuka, A.; Kim, D. Reversal of Hückel (Anti)Aromaticity in the Lowest Triplet States of Hexaphyrins and Spectroscopic Evidence for Baird's Rule, *Nat. Chem.* **2015**, *7*, 418-422.

13 Rosenberg, M.; Dahlstrand, C.; Kilså, K.; Ottosson, H. Excited State Aromaticity and Antiaromaticity: Opportunities for Photophysical and Photochemical Rationalizations. *Chem. Rev.* **2014**, *114*, 5379–5425.

14 Papadakis, R.; Ottosson, H. The Excited State Antiaromatic Benzene Ring: A Molecular Mr Hyde? *Chem. Soc. Rev.* **2015**, *44***,** 6472–6493.

15 Oh, J.; Sung, Y. M.; Hong, Y.; Kim, D. Spectroscopic Diagnosis of Excited-State Aromaticity: Capturing Electronic Structures and Conformations upon Aromaticity Reversal. *Acc. Chem. Res.* **2019**, *51*, 1349–1358.

16 Jorner, K. Baird Aromaticity in Excited States and Open-Shell Ground States. *Aromaticity*, Elsevier, Israel Fernández (editor), **2021**, 375–405.

17 Aihara, J. Three-Dimensional Aromaticity of Polyhedral Boranes, *J. Am. Chem. Soc.* **1978**, *100*, 3339–3342.

18 Lipscomb, W. N.; Pitochelli, A. R.; Hawthorne, M. F. Probable Structure of the $B_{10}H_{10}^{-2}$ Ion, *J. Am. Chem. Soc.* **1959**, *81*, 5833 – 5834.

19 Wade, K. The Structural Significance of the Number of Skeletal Bonding Electron-Pairs in Carboranes, the Higher Boranes and Borane Anions, and Various Transition-Metal Carbonyl Cluster Compounds, *J. Chem. Soc. D Chem. Comm.* **1971**, 792-793.

20 Mingos, D. M. P. Polyhedral Skeletal Electron Pair Approach, *Acc. Chem. Res.* **1984,** *17*, 311-319.

21 Poater, J.; Viñas, C.; Bennour, I.; Escayola, S.; Solà, M.; Teixidor, F. Too Persistent to Give Up: Aromaticity in Boron Clusters Survives Radical Structural Changes, *J. Am. Chem. Soc.* **2020**, *142*, 9396-9407.

22 Pitt, M. P.; Paskevicius, M.; Brown, D. H.; Sheppard, D. A.; Buckley, C. E. Thermal Stability of $Li_2B_{12}H_{12}$ and Its Role in the Decomposition of $LiBH_4$. *J. Am. Chem. Soc.* **2013**, *135*, 6930–6941.

23 Udovic, T. J.; Matsuo, M.; Unemoto, A.; Verdal, N.; Stavila, V.; Skripov, A. V; Rush, J. J.; Takamura, H.; Orimo, S. Sodium Superionic Conduction in $Na_2B_{12}H_{12}$. *Chem. Commun.* **2014**, *50*, 3750–3752.

24 King, R. B. Three-Dimensional Aromaticity in Polyhedral Boranes and Related Molecules. *Chem. Rev.* **2001**, *101*, 1119–1152.

25 Garcia-Borràs, M.; Osuna, S.; Luis, J. M.; Swart, M.; Solà, M. The Role of Aromaticity in Determining the Molecular Structure and Reactivity of (Endohedral Metallo)Fullerenes. *Chem. Soc. Rev.* **2014**, *43*, 5089–5105.

26 El Bakouri, O.; Duran, M.; Poater, J.; Feixas, F.; Solà, M. Octahedral Aromaticity in $^{2S+1}A_{1g}$ X_6^q Clusters (X = Li–C and Be–Si, S = 0–3, and q = −2 to +4). *Phys. Chem. Chem. Phys.*, **2016**, *18*, 11700–11706.

27 Hirsch, A.; Chen, Z.; Jiao, H. Spherical Aromaticity in I_h Symmetrical Fullerenes: The $2(N+1)^2$ Rule. *Angew. Chem. Int. Ed.*, **2000**, *39*, 3915–3917.

28 Hirsch, A.; Chen, Z.; Jiao, H. Spherical Aromaticity of Inorganic Cage Molecules. *Angew. Chem. Int. Ed.* **2001**, *40*, 2834–2838.

29 Liu, C.; Popov, I. A.; Chen, Z.; Boldyrev, A. I.; Sun; Z. M. Aromaticity and Antiaromaticity in Zintl Clusters. *Chem. - A Eur. J.* **2018**, *24*, 14583–14597.

30 Cui, P.; Hu, H.-S.; Zhao, B.; Miller, J. T.; Cheng, P.; Li, J. A Multicentre-Bonded $[Zn^I]_8$ Cluster with Cubic Aromaticity. *Nat. Commun.* **2015**, *6*, 6331.

31 Corminboeuf, C.; Schleyer, P. v. R.; Warner, P. Are Antiaromatic Rings Stacked Face-to-Face Aromatic? *Org. Lett.* **2007**, *9*, 3263–3266.

32 Nozawa, R.; Kim, J.; Oh, J.; Lamping, A.; Wang, Y.; Shimizu, S.; Hisaki, I.; Kowalczyk, T.; Fliegl, H.; Kim, D.; Shinokubo, H. Three-Dimensional Aromaticity in an Antiaromatic Cyclophane. *Nat. Commun.* **2019**, *10*, 1–7.

33 Kim, G.; Dutta, R.; Cha, W.; Hong, S.; Oh, J.; Firmansyah, D.; Jo, H.; Ok, K. M.; Lee, C.; Kim, D. Noncovalent Intermolecular Interaction in Cofacially Stacked 24π Antiaromatic Hexaphyrin Dimer, *Chem. Eur. J.* **2020**, *26*, 16434–16440.

34 Kawashima, H.; Ukai, S.; Nozawa, R.; Fukui, N.; Fitzsimmons, G.; Kowalczyk, T.; Fliegl, H.; Shinokubo, H. Determinant Factors of Three-Dimensional Aromaticity in Antiaromatic Cyclophanes. *J. Am. Chem. Soc.* **2021**, *143*, 10676–10685.

35 Ni, Y.; Gopalakrishna, T. Y.; Phan, H.; Kim, T.; Herng, T. S.; Han, Y.; Tao, T.; Ding, J.; Kim, D.; Wu, J. 3D Global Aromaticity in a Fully Conjugated Diradicaloid Cage at Different Oxidation States. *Nat. Chem.* **2020**. *12*, 242–248.

36 Casado, J.; Martín, N. The New "Noble Gas" Molecule: A Molecular Trip beyond Atoms. *Chem* **2020**, *6*, 1514–1516.

37 Cha, W.-Y.; Kim, T.; Ghosh, A.; Zhang, Z.; Ke, X.-S.; Ali, R.; Lynch, V. M.; Jung, J.; Kim, W.; Lee, S.; Fukuzumi, S.; Park, J. S.; Sessler, J. L.; Chandrashekar, T. K.; Kim, D. Bicyclic Baird-Type Aromaticity. *Nat. Chem.* **2017**, *9*, 1243–1248.

38 Goldstein, M. J. Bicycloaromaticity. 4m + 2, 4n rule. *J. Am. Chem. Soc.* **1967**, *89*, 6357–6359.

39 Valiev, R. R.; Fliegl, H.; Sundholm, D. Bicycloaromaticity and Baird-Type Bicycloaromaticity of Dithienothiophene-Bridged [34]octaphyrins. *Phys. Chem. Chem. Phys.* **2018**, *20*, 17705–17713.

40 Goldstein, M. J.; Hoffmann, R. Symmetry, Topology and Aromaticity, *J. Am. Chem. Soc.*, **1971**, *93*, 6193-6204.

41 Fokin, A. A.; Kiran, B.; Bremer, M.; Yang, X.; Jiao, H.; Schleyer, P. v. R.; Schreiner, P. R. Which Electron Count Rules Are Needed for Four-Center Three-Dimensional Aromaticity? *Chem. Eur. J.* **2000**, *6*, 1615–1628.

42 Bultinck, P.; Fias, S.; Ponec, R. Local Aromaticity in Polycyclic Aromatic Hydrocarbons: Electron Delocalization versus Magnetic Indices. *Chem. Eur. J.* **2006**, *12*, 8813–8818.

43 Bultinck, P. A Critical Analysis of the Local Aromaticity Concept in Polyaromatic Hydrocarbons. *Faraday Discussions*, **2007**, *135*, 347-365.

44 Fias, S.; Fowler, P.; Delgado, J.L.; Hahn, U.; Bultinck, P. Correlation of Delocalization Indices and Current-Density Maps in Polycyclic Aromatic Hydrocarbons. *Chem. Eur. J.*, **2008**, *14*, 3093-3099.

45 Fias, S.; Damme, S. V.; Bultinck, P. Multidimensionality of Delocalization Indices and Nucleus Independent Chemical Shifts in Polycyclic Aromatic Hydrocarbons. *J. Comput. Chem.*, **2008**, *29*, 358-356.

46 Fias, S.; Damme, S. V.; Bultinck, P. Multidimensionality of Delocalization Indices and Nucleus-Independent Chemical Shifts in Polycyclic Aromatic Hydrocarbons II: Proof of Further Nonlocality. *J. Comput. Chem.*, **2010**, *31*, 2286-2893.

47 Szczepanik, D. W.; Solà, M.; Krygowski, T. M.; Szatylowicz, H.; Andrzejak, M.; Pawełek, B.; Dominikowska, J.; Kukułka, M.; Dyduch, K. Aromaticity of Acenes: The Model of Migrating π-Circuits. *Phys. Chem. Chem. Phys.*, **2018**, *20*, 13430–13436.

48 Bühl, M.; Hirsch, A. Spherical Aromaticity of Fullerenes. *Chem. Rev.* **2001**, *101*, 1153–1184.

49 Chen, Z.; Wu, J. I.; Corminboeuf, C.; Bohmann, J.; Lu, X.; Hirsch, A.; Schleyer, P. von R. Is C_{60} Buckminsterfullerene Aromatic? *Phys. Chem. Chem. Phys.* **2012**, *14*, 14886–14891.

50 Wasserman, E.; Hutton, R. S.; Kuck, V. J.; Chandross, E. A. Dipositive Ion of Hexachlorobenzene. A Ground-State Triplet. *J. Am. Chem. Soc.* **1974**, *96*, 1965-1966.

51 Ebata, K.; Setaka, W.; Inoue, T.; Kabuto, C.; Kira, M.; Sakurai, H. Planar Hexasilylbenzene with Thermally Accesible Triplet State, *J. Am. Chem. Soc.* **1998**, *120*, 1335-1336.

52 Gould, C. A.; Marbey, J.; Vieru, V.; Marchiori, D. A.; David Britt, R.; Chibotaru, L. F.; Hill, S.; Long, J. R. Isolation of a Triplet Benzene Dianion. *Nat. Chem.* **2021**, *13*, 1001–1005.

53 J. Ren, L.; Han, Y.; Hou, X.; Ni, Y.; Wu, J. All Are Aromatic: A 3D Globally Aromatic Cage Containing Five Types of 2D Aromatic Macrocycles. *Chem* **2021**, *7*, DOI: doi.org/10.1016/j.chempr.2021.11.003

54 Becke, A.D. Density-Functional Thermochemistry. III. The Role of Exact Exchange, *J. Chem. Phys.* **1993**, *98*, 5648-5652.

55 Stephens, P. J.; Devlin, F. J.; Chabalowski, C. F.; Frisch, M. J. Ab Initio Calculation of Vibrational Absorption and Circular Dichroism Spectra Using Density Functional Force Fields. *J. Phys. Chem.* **1994**, *98*, 11623– 11627.

56 Lee, C.; Yang, W.; Parr, R. G. Development of the Colle-Salvetti Correlation-Energy Formula into a Functional of the Electron Density. *Phys. Rev. B*, **1988**, *37*, 785–789.

57 Yanai, T.; Tew, D. P.; Handy, N. C. A New Hybrid Exchange-Correlation Functional Using the Coulomb-Attenuating Method (CAM-B3LYP). *Chem. Phys. Lett.* **2004**, *393*, 51– 57.

58 Casademont-Reig, I.; Woller, T.; Contreras-García, J.; Alonso, M.; Torrent-Sucarrat, M.; Matito, E. New Electron Delocalization Tools to Describe the Aromaticity in Porphyrinoids. *Phys. Chem. Chem. Phys.* **2018**, *20*, 2787–2796.

59 Szczepanik, D. W.; Solà, M.; Andrzejak, M.; Pawełek, B.; Dominikowska, J.; Kukułka, M.; Dyduch, K.; Krygowski, T. M.; Szatylowicz, H. The Role of the Long-Range Exchange Corrections in the Description of Electron Delocalization in Aromatic Species. *J. Comput. Chem.*, **2017**, *38*, 1640–1654.

60 Szczepanik, D. W.; Andrzejak, M.; Dyduch, K.; Żak, E.; Makowski, M.; Mazur, G.; Mrozek, J. A Uniform Approach to the Description of Multicenter Bonding, *Phys. Chem. Chem. Phys.*, **2014**, *16*, 20514-20523.

61 Szczepanik, D. W.; Andrzejak, M.; Dominikowska, J.; Pawełek, B.; Krygowski, T. M.; Szatylowicz, H.; Solà, M. The Electron Density of Delocalized Bonds (EDDB) Applied for Quantifying Aromaticity, *Phys. Chem. Chem. Phys.*, **2017**, *19*, 28970–28981.

62 Schleyer, P. v. R.; Maerker, C.; Dransfeld, A.; Jiao, H.; van Eikema Hommes, N. J. R. Nucleus-Independent Chemical Shifts: A Simple and Efficient Aromaticity Probe. *J. Am. Chem. Soc.*, **1996**, *118*, 6317–6318.

63 Chen, Z.; Wannere, C. S.; Corminboeuf, C.; Puchta, R.; Schleyer, P. v. R. Nucleus-Independent Chemical Shifts (NICS) as an Aromaticity Criterion, *Chem. Rev.* **2005**, *105*, 3842-3888.

64 Stanger, A. Nucleus-Independent Chemical Shifts (NICS): Distance Dependence and Revised Criteria for Aromaticity and Antiaromaticity, *J. Org. Chem.*, **2006**, *71*, 883-893.

65 Gershoni-Poranne, R.; Stanger, A. The NICS-XY-Scan: Identification of Local and Global Ring Currents in Multi-Ring Systems, *Chem. Eur. J.*, **2014**, *20*, 5673-5688.

66 Geuenich, D.; Hess, K.; Köhler, F.; Herges, R. Anisotropy of the Induced Current Density (ACID), a General Method To Quantify and Visualize Electronic Delocalization, *Chem. Rev.*, 2005, **105**, 3758-3772.

67 Fliegl, H.; Taubert, S.; Lehtonen, O.; Sundholm, D. The Gauge Including Magnetically Induced Current Method, *Phys. Chem. Chem. Phys.*, **2011**, *13*, 20500–20518.

68 Murrell, J. N., Harget, A. J., Semi-Empirical Self-Consistent-Field Molecular Orbital Theory of Molecules, 1972, Wiley-Interscience, New York.

69 Peeks, M. D.; Claridge, T. D. W.; Anderson, H. L. Aromatic and Antiaromatic Ring Currents in a Molecular Nanoring. *Nature* **2017**, *541*, 200–203.

70 Frisch, M. J.; Trucks, G. W.; Schlegel, H. B.; Scuseria, G. E.; Robb, M. A.; Cheeseman, J. R.; Scalmani, G.; Barone, V.; Mennucci, B.; Petersson, G. A.; Nakatsuji, H.; Caricato, M.; Li, X.; Hratchian, H. P.; Izmaylov, A. F.; Bloino, J.; Zheng, G.; Sonnenberg, J. L.; Hada, M.; Ehara, M.; Toyota, K.; Fukuda, R.; Hasegawa, J.; Ishida, M.; Nakajima, T.; Honda, Y.; Kitao, O.; Nakai, H.; Vreven, T.; Montgomery, Jr., J. A.; Peralta, J. E.; Ogliaro, F.; Bearpark, M.; Heyd, J. J.; Brothers, E.; Kudin, K. N.; Staroverov, V. N.; Kobayashi, R.; Normand, J.; Raghavachari, K.; Rendell, A.; Burant, J. C.; Iyengar, S. S.; Tomasi, J.; Cossi, M.; Rega, N.; Millam, J. M.; Klene, M.; Knox, J. E.; Cross, J. B.; Bakken, V.; Adamo, C.; Jaramillo, J.; Gomperts, R.; Stratmann, R. E.; Yazyev, O.;

Austin, A. J.; Cammi, R.; Pomelli, C.; Ochterski, J. W.; Martin, R. L.; Morokuma, K.; Zakrzewski, V. G.; Voth, G. A.; Salvador, P.; Dannenberg, J. J.; Dapprich, S.; Daniels, A. D.; Farkas, Ö.; Foresman, J. B.; Ortiz, J. V.; Cioslowski, J. and; Fox, D. J. Gaussian 16. Gaussian Inc.: Wallingford CT 2016.

71 E. D. Glendening, A. E. Reed, J. E. Carpenter and F. Weinhold, NBO 3.1, TCI, University of Wisconsin, Madison, 1998.

72 Avogadro: An Open-Source Molecular Builder and Visualization Tool. Version 1.2.0.

73 Hanwell, M. D.; Curtis, D. E.; Lonie, D. C.; Vandermeersch, T.; Zurek, E.; Hutchison, G. R. Avogadro: an advanced semantic chemical editor, visualization, and analysis platform, *J. Cheminform.*, **2012**, *4*, 17.

74 Rahalkar, A. P.; Stanger, A. "Aroma" https://chemistry.technion.ac.il/members/amnon-stanger/

75 Herges, R.; Geuenich, D. Delocalization of Electrons in Molecules. *J. Phys. Chem. A* **2001**, *105*, 3214 – 3220.

76 Geuenich, D.; Hess, K.; Köhler, F.; Herges, R. Anisotropy of the Induced Current Density (ACID), a General Method To Quantify and Visualize Electronic Delocalization. *Chem. Rev.* **2005**, *105*, 3758 - 3772.

For Table of Contents Only